

# Hybrid density functional theory study of fragment ions generated during mass spectrometry of 1,3-dioxane derivatives

Titus V. Albu\*

Department of Chemistry, Box 5055, Tennessee Technological University, Cookeville, Tennessee 38505, USA

Received 22 February 2006; Revised 7 April 2006; Accepted 10 April 2006

**It was recently reported that the *cis,cis* and *trans,trans* diastereoisomers of four 2(*r*)-R-2,4(*R*),6(*S*)-trimethyl-1,3-dioxane derivatives show distinct electron ionization mass spectra. As a possible explanation for this finding, the authors suggested that the ions generated during the mass spectrometry of these compounds could follow different fragmentation patterns that initiate from different ion conformations. In this report, hybrid density functional theory methods have been used to investigate the conformational preference of three ions involved in the mass spectrometry of some 1,3-dioxane derivatives. We found that there is indeed more than one stable ion conformation for each of the investigated ions. Energy profiles along the torsional coordinates connecting the conformers are presented, and factors influencing the relative stability of ion conformations are discussed.**

Copyright © 2006 John Wiley & Sons, Ltd.

Electron ionization mass spectrometry (EI-MS) is a useful tool in structural investigation of organic compounds. The method has, however, some limitations due to its lack of discrimination between stereoisomers, which typically show very similar mass spectra. Analysis of stereoisomers is usually carried out by other MS techniques,<sup>1,2</sup> and examples of these techniques being used to discriminate between enantiomers or diastereoisomers have been reported for a variety of classes of organic substances.<sup>3–13</sup> There are only a limited number of studies presenting differences in the EI mass spectra of diastereoisomers in saturated six-membered ring derivatives.<sup>14–16</sup>

In a recent communication, Loutelier-Bourhis *et al.*<sup>16</sup> reported important differences in the abundances of fragment ions obtained in mass spectrometry of the *cis,cis* and *trans,trans* diastereoisomers of four 2(*r*)-R-2,4(*R*),6(*S*)-trimethyl-1,3-dioxane derivatives. To explain the large differences observed between the EI mass spectra of these diastereoisomers, the authors propose, as one possibility, the formation of two pairs of isomeric ions by the loss of the substituent located in the equatorial or axial position at C(2), respectively. These isomeric ions were postulated to exhibit large differences in their stabilities.

The existence of more than one stable conformation for carbocations has previously been determined for other cyclic systems. In a theoretical study, Rauk *et al.*<sup>17</sup> established the presence of two distinct conformers for the 1-methyl-1-cyclohexyl cation, both isomers having the chair conformation. The presence of these two conformers explained the observation of distinct  $\beta$ -<sup>13</sup>C NMR chemical shifts in solution.<sup>18</sup> Rauk *et al.*<sup>17</sup> used MP2/6-31G(d) and B3LYP/6-31G(d) levels of theory in that study but did not investigate in detail the process of interchange between the two conformers or its energetics. More recently, Alabugin and Manoharan carried out a systematic computational study into the stability of  $\delta$ -substituted cyclohexyl cations.<sup>19</sup>

In this report, we present the results of a hybrid density functional theory study into the conformations of some ions obtained in the initial stages of the fragmentation process in mass spectroscopy of *cis,cis* and *trans,trans* diastereoisomers of 2(*r*)-chloromethyl-2,4(*R*),6(*S*)-trimethyl-1,3-dioxane (1, Fig. 1) and 2(*r*)-ethyl-2,4(*R*),6(*S*)-trimethyl-1,3-dioxane (2, Fig. 1). The purpose of this study is two-fold because we investigate not only the existence of more than one stable conformer for the ions generated during the mass spectroscopy of the selected substituted dioxanes, but also the energetics of the interchange process in order to determine if the conformers might present different reactivities leading to different fragmentation processes.

\*Correspondence to: T. V. Albu, Department of Chemistry, Box 5055, Tennessee Technological University, Cookeville, Tennessee 38505, USA.  
E-mail: albu@tntech.edu  
Contract/grant sponsor: College of Arts and Sciences at Tennessee Technological University.

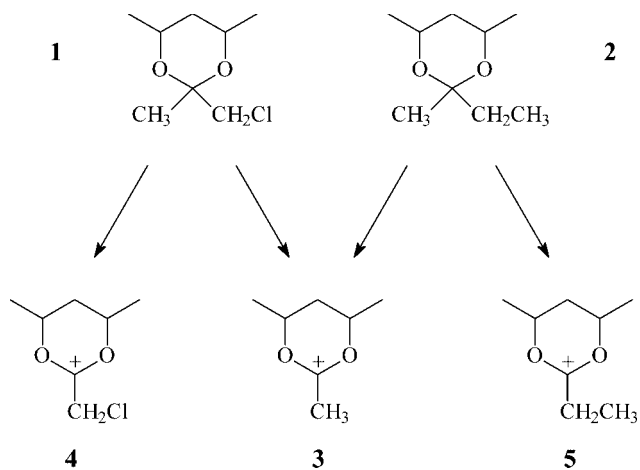


**Figure 1.** The initial 2,2,4,6-tetrasubstituted 1,3-dioxane derivatives (**1** and **2**) and the ions (**3**, **4**, and **5**) generated during their fragmentation process in mass spectrometry.

## COMPUTATIONAL METHODOLOGIES

In this study, we used mPW1PW91<sup>20,21</sup> and MPW1K<sup>22</sup> hybrid density functional theory methods in conjunction with the 6-31+G(d,p) basis set. Generally, the one-parameter hybrid Fock-Kohn-Sham operator can be written as:

$$F = F^H + (X/100)F^{HFE} + [1 - (X/100)](F^{SE} + F^{GCE}) + F^C$$

where  $F^H$  is the Hartree operator (i.e., the nonexchange part of the Hartree-Fock operator),  $F^{HFE}$  is the Hartree-Fock (HF) exchange operator,  $X$  is the fraction of Hartree-Fock exchange,  $F^{SE}$  is the Dirac-Slater local density functional for exchange,  $F^{GCE}$  is the gradient correction for the exchange functional, and  $F^C$  is the total correlation functional including both local and gradient-corrected parts. For both methods used in this study,  $F^{GCE}$  is the mPW functional of Adamo and Barone,<sup>21</sup> and  $F^C$  is the PW91 correlation functional.<sup>20</sup> The difference between the two methods is in the contribution of Hartree-Fock exchange functional, with  $X=25$  for mPW1PW91 and  $X=42.8$  for MPW1K,<sup>22</sup> respectively.

All systems were closed-shell systems, and we employed restricted wave function calculations. We carried out the geometry optimizations using a tight convergence criteria and an ultrafine integration grid for numerical integrations. All electronic structure calculations were carried out using Gaussian 03 program.<sup>23</sup>

## RESULTS

The three ions investigated in this study are the cations **3**, **4**, and **5** shown in Fig. 1. The main focus of the study is to investigate the ion conformations obtained by the rotation along the C(2)–C(7) single bond and their relative stabilities. The choice of the dihedral angle that can be used to monitor the rotation along this single carbon–carbon bond is not unique. We chose to investigate the energy profile along a torsional coordinate using the dihedral angle defined by C(5), C(2), C(7) and Z (where Z is H in **3**, Cl in **4**, and C of CH<sub>3</sub> in **5**) as the geometric parameter to monitor this coordinate (Fig. 2). This dihedral angle is preferred because the conformers obtained for dihedral angles of 0° and 180° have

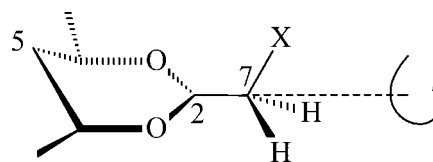


**Figure 2.** The definition of the torsional coordinate.

$C_s$  symmetry, and because they are also minima along this torsional coordinate. In the rest of the paper, we will refer to this dihedral angle as the CCCZ dihedral angle or, simply, the torsional coordinate.

The results of our calculations are presented in Figs. 3, 4, and 5 and in Tables 1, 2 and 3. The three figures show the energy profiles along the torsional coordinate that interchanges the investigated conformers for each of the three fragment ions examined. We obtained the energy profile in these figures, by maintaining the torsional coordinate fixed while fully optimizing all the other internal coordinates. In Figs. 3–5, we choose to represent only the potential between 0 and 180° because, due to the symmetry of each system, the whole torsional potential can be created based on the part represented in these figures. One can determine the energy at other dihedral angles either using  $E(\theta) = E(-\theta)$  or using  $E(180 - \theta) = E(180 + \theta)$ , where  $E(x)$  is the electronic energy at a CCCZ dihedral angle equal to  $x$ .

In Tables 1–3, we present selected geometric and energetic parameters for the stationary points (i.e., minima and saddle points) obtained for the three ions examined here. In these tables,  $\theta$  represents the torsional coordinate,  $R$  represents a bond distance involving C(7),  $V$  represents the electronic (i.e., zero-point-exclusive) energy relative to the lowest electronic energy obtained among all investigated ion conformations, and  $\Delta G_{298}$  represents the free energy at 298 K relative to the lowest such quantity among all investigated conformers. In calculating  $\Delta G_{298}$ , the rigid rotor-harmonic oscillator approximation was employed. Finally,  $\omega$  represents either the lowest frequency (if the structure is a minimum) or the imaginary frequency (if the structure is a saddle point). This frequency is a good indication of the local shape of the potential energy along the torsional coordinate.

## DISCUSSION

We initially carried out an extensive study using the mPW1PW91/6-31+G(d,p) level of theory, which is an excellent method for investigating molecular properties like the geometry and the vibrational frequencies. In order to investigate the dependence of our results on the theoretical method used, we choose to carry out limited calculations (i.e., for the stationary points only) using a second method. We choose the MPW1K/6-31+G(d,p) level of theory, which is a method designed for use in kinetic studies. The MPW1K hybrid density functional method has been shown to give good energetics for barrier heights and good geometries for reactive saddle points,<sup>24–27</sup> and has been used effectively in direct dynamics studies.<sup>28,29</sup> Comparing the results from the two methods will also allow us to investigate the effect of the HF exchange contribution on the results.

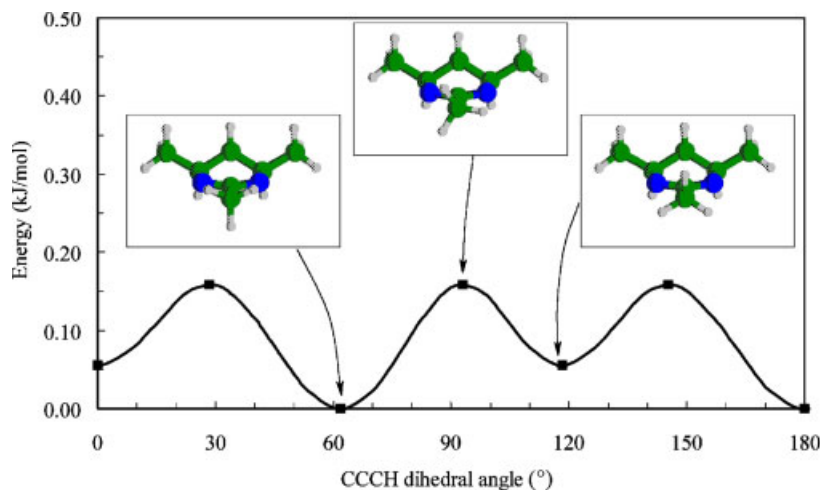


**Figure 3.** Torsional coordinate for  $[C_5H_{10}O_2-CH_3]^+$  (**3**) calculated at the mPW1PW91/6-31+G(d,p) level of theory. The stationary points along this coordinate are shown inset.

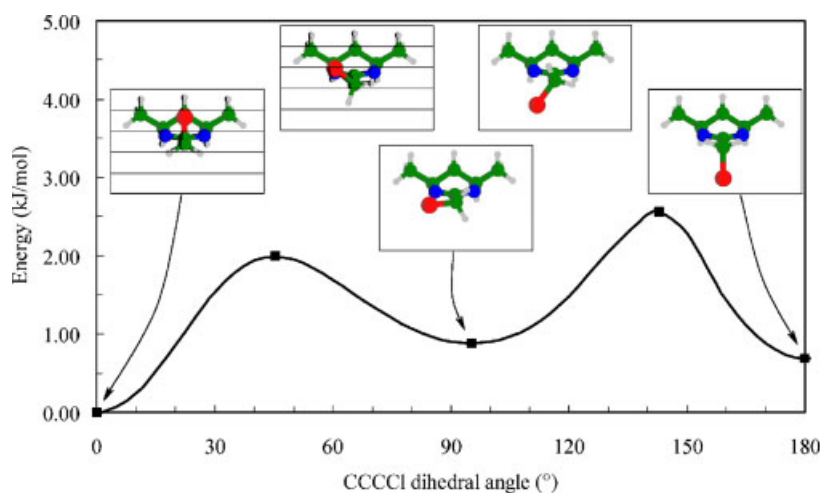


**Figure 4.** Torsional coordinate for  $[C_5H_{10}O_2-CH_2Cl]^+$  (**4**) calculated at the mPW1PW91/6-31+G(d,p) level of theory. The stationary points along this coordinate are shown inset.

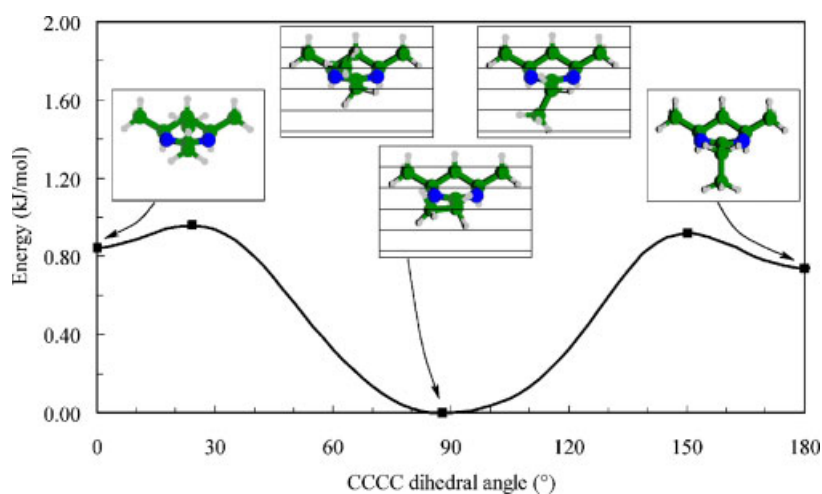


**Figure 5.** Torsional coordinate for  $[C_5H_{10}O_2-CH_2CH_3]^+$  (**5**) calculated at the mPW1PW91/6-31+G(d,p) level of theory. The stationary points along this coordinate are shown inset.

**Table 1.** Geometric and energetic parameters for the stationary points along the torsional coordinate for  $[\text{C}_5\text{H}_{10}\text{O}_2\text{-CH}_3]^+$  (**3**)

Method	$\theta^a$ (°)			$R_{\text{C-H}}^b$ (Å)			$V$ (kJ/mol)	$\Delta G$ (kJ/mol)	$\omega$ (cm <sup>-1</sup> )
mPW1PW91/6-31+G(d,p)	0.0	118.3	-118.3	1.096	1.089	1.089	0.06	0.00	41.5
	28.4	145.3	-93.0	1.093	1.093	1.087	0.16	4.14	45.2 <i>i</i>
	61.8	180.0	-61.8	1.089	1.096	1.089	0.00	0.23	46.4
MPW1K/6-31+G(d,p)	0.0	118.2	-118.2	1.090	1.084	1.084	0.07	0.00	43.6
	27.8	144.7	-93.6	1.088	1.088	1.082	0.18	4.01	47.1 <i>i</i>
	61.8	180.0	-61.8	1.084	1.091	1.084	0.00	0.26	49.7

<sup>a</sup>  $\theta$  is the CCCH dihedral angle (i.e., the torsional coordinate).

<sup>b</sup> The C-H distances correspond to the CCCH dihedral angles listed three columns to the left.

**Table 2.** Geometric and energetic parameters for the stationary points along the torsional coordinate for  $[\text{C}_5\text{H}_{10}\text{O}_2\text{-CH}_2\text{Cl}]^+$  (**4**)

Method	$\theta^a$ (°)	$R_{\text{C-Cl}}$ (Å)	$R_{\text{C-H}}$ (Å)	$R_{\text{C-H}}$ (Å)	$V$ (kJ/mol)	$\Delta G$ (kJ/mol)	$\omega$ (cm <sup>-1</sup> )
mPW1PW91/6-31+G(d,p)	0.0	1.780	1.089	1.089	0.00	1.41	32.1
	45.5	1.768	1.094	1.089	1.99	7.46	31.7 <i>i</i>
	95.3	1.755	1.094	1.093	0.88	0.00	23.7
	143.0	1.768	1.089	1.094	2.56	8.07	33.8 <i>i</i>
	180.0	1.780	1.089	1.089	0.69	2.10	33.5
MPW1K/6-31+G(d,p)	0.0	1.767	1.084	1.084	0.00	1.78	31.0
	40.8	1.757	1.088	1.083	1.61	7.63	32.1 <i>i</i>
	95.9	1.744	1.089	1.088	0.06	0.00	27.0
	145.3	1.757	1.083	1.088	2.21	8.27	33.4 <i>i</i>
	180.0	1.767	1.084	1.084	0.69	2.49	32.5

<sup>a</sup>  $\theta$  is the CCCCl dihedral angle (i.e., the torsional coordinate).

**Table 3.** Geometric and energetic parameters for the stationary points along the torsional coordinate for  $[\text{C}_5\text{H}_{10}\text{O}_2\text{-CH}_2\text{CH}_3]^+$  (**5**)

Method	$\theta^a$ (°)	$R_{\text{C-C}}$ (Å)	$R_{\text{C-H}}$ (Å)	$R_{\text{C-H}}$ (Å)	$V$ (kJ/mol)	$\Delta G$ (kJ/mol)	$\omega$ (cm <sup>-1</sup> )
mPW1PW91/6-31+G(d,p)	0.0	1.540	1.092	1.092	0.84	2.43	18.1
	24.3	1.537	1.095	1.090	0.96	8.51	21.1 <i>i</i>
	87.8	1.521	1.098	1.096	0.00	0.00	15.1
	150.2	1.536	1.090	1.096	0.92	8.42	21.0 <i>i</i>
	180.0	1.541	1.092	1.092	0.74	2.46	19.7
MPW1K/6-31+G(d,p)	0.0	1.533	1.086	1.086	1.25	2.16	15.9
	19.1	1.530	1.089	1.085	1.31	8.55	16.8 <i>i</i>
	89.0	1.515	1.092	1.091	0.00	0.00	17.4
	154.1	1.530	1.085	1.090	1.24	8.45	19.5 <i>i</i>
	180.0	1.533	1.086	1.086	1.13	2.35	18.5

<sup>a</sup>  $\theta$  is the CCCC dihedral angle (i.e., the torsional coordinate).

For the  $[\text{C}_5\text{H}_{10}\text{O}_2\text{-CH}_3]^+$  ion (**3**), we found a total of six minima along the torsional coordinate between 0 and 360°. Three of these minima are equivalent, and so are the other three. We therefore choose to characterize only one minimum of each type in Table 1. The barrier height for methyl rotation in **3**, that converts one stable conformer into the other, is calculated to be very small (less than 0.20 kJ/mol) using both electronic structure theory methods. This very small barrier of rotation implies that the methyl group should rotate freely at room temperature (RT = 2.48 kJ/mol at 298 K).

For both the  $[\text{C}_5\text{H}_{10}\text{O}_2\text{-CH}_2\text{Cl}]^+$  (**4**) and the  $[\text{C}_5\text{H}_{10}\text{O}_2\text{-CH}_2\text{CH}_3]^+$  (**5**) ions, we found only four minima along the torsional coordinate, one having a CCCZ dihedral angle of 0°, one having a CCCZ dihedral angle of 180°, and two equivalent ones with CCCZ dihedral angles of about 90°

and -90°, respectively. In the following discussion we will label these three distinct conformers as 0-deg conformer, 180-deg conformer, and 90-deg conformer, respectively. In the case of ion **4**, the lowest-energy conformer is the 0-deg conformer (Table 2), while for ion **5** the lowest-energy conformer is the 90-deg conformer (Table 3).

Comparing the results obtained with the two methods used in this study, one can observe that the MPW1K method gives an increased preference for the 90-deg conformer for both **4** and **5**. For cation **4**, mPW1PW91 functional predicts that the highest-energy stable conformer is the 90-deg one while MPW1K functional predicts that the energy of the 90-deg conformer is very close to the energy of the 0-deg conformer (which is the lowest-energy conformer). This is accompanied by a reduction in the barrier height for the rotation along the C(2)-C(7) bond using the MPW1K

functional. For cation **5**, the 90-deg conformer is the lowest-energy conformer for both methods but is more stable than the 0-deg and 180-deg conformers using the MPW1K method. In this case, the barrier of rotation increases and the CCCZ dihedral angles for the saddle points along the torsional coordinate are further apart from each other and closer to 0 and 180°. (The CCCZ dihedral angles are 24.3 and 150.2° using mPW1PW91 versus 19.1 and 154.1° using MPW1K.) It is interesting to note that considering the Gibbs free energy ( $\Delta G$ ), the 90-deg conformer is the most stable isomer for both cations **4** and **5**, and using both methods (Tables 2 and 3).

One can also discover a good correlation between the calculated vibrational frequency and the energy profile along the torsional coordinate for all ion conformations examined. Comparing mPW1PW91 and MPW1K results, the higher vibrational frequencies (both positive for minima and imaginary for saddle points) correlate well with the relative stability of the conformers for all three ions examined.

In order to understand the existence and the relative stability of the three types of conformers for **4** and **5**, a more careful analysis is necessary. Our calculations show that, for all conformations of all three fragment ions, the three bonds that C(2) is making with O(1), O(3), and C(7) are almost coplanar. This corresponds to an  $sp^2$  hybridization for C(2) and the existence of an empty  $p$  orbital on C(2). As a result, the relative stabilities of different conformers for the ions examined can be better understood by investigating the possible ways of stabilizing the empty  $p$  orbital at C(2).

Within valence bond theory,<sup>30</sup> the main factor for the overall stability of the ions is the mesomeric stabilization (i.e., resonance) between the empty  $p$  orbital on C(2) and lone pairs of the two oxygen atoms in the ring. However, this stabilization is present for all conformers and all ions and will not influence significantly the conformer relative stability. Consequently, this relative stability will be determined primarily by the different hyperconjugative stabilization occurring between the empty  $p$  orbital and the three  $\sigma$  bonds at C(7), other than that with C(2), which will further stabilize the  $p$  orbital. This stabilizing hyperconjugation<sup>30</sup> is more significant when a  $\sigma$  bond is parallel (or close to parallel) to the empty  $p$  orbital and of no consequence when a  $\sigma$  bond is perpendicular to the empty  $p$  orbital. When hyperconjugation is occurring, the  $\sigma$  bond becomes weaker and therefore longer. Similarly, when hyperconjugation is not present, the  $\sigma$  bond is stronger and therefore shorter. A simple method of monitoring the extent of hyperconjugative stabilization of the empty  $p$  orbital at C(2) is to investigate systematically the internuclear distances between C(7) and the atoms bonded to it.

The results in Tables 2 and 3 show clearly that there are significant changes in bond lengths between C(7) and Cl (for **4**) and between C(7) and C(8) (for **5**) when comparing the conformers in which those bonds are involved in hyperconjugation (0-deg and 180-deg conformers) with the 90-deg conformer in which the hyperconjugation is insignificant. For example, using the mPW1PW91 method, the C–Cl bond in **4** decreases from 1.780 Å in both the 0-deg and 180-deg conformers to 1.755 Å in the 90-deg conformer (Table 2). The

change is slightly less using the MPW1K method but still significant.

For ion **4**, as the C–Cl distance decreases when going from the 0-deg conformer to the 90-deg conformer, both C(7)–H distances increase. The 90-deg conformer is asymmetric so the C–H distances are not exactly the same but they are very close in value at 1.094 and 1.093 Å, respectively. A similar behavior is observed for the C(7)–H bond distances in ion **5**. The MPW1K method gives slightly shorter distances than the mPW1PW91 method but similar changes when comparing the conformers. A good correlation between the C–H bond lengths and the presence of hyperconjugation is also present for cation **3**, with a longer C–H distance for a torsional coordinate of 0 or 180° (equivalent to a C–H  $\sigma$  bond parallel to the empty  $p$  orbital).

Considering all the above, the determining factor in the relative stabilities of the conformers for the ions **4** and **5** appears to be the ability of the C–Cl and C–C  $\sigma$  bonds to stabilize through hyperconjugation the empty  $p$  orbital at C(2). For cation **4**, hyperconjugation with the C–Cl bond stabilizes well the  $p$  orbital in the 0-deg and the 180-deg conformers where this bond is parallel to this empty  $p$  orbital. In the 90-deg conformer this interaction is almost completely absent so the only stabilization is hyperconjugation with the two C–H bonds, which is less efficient, leading to a higher-energy conformer. For cation **5**, hyperconjugation with the C–C bond does not stabilize well the empty  $p$  orbital in the 0-deg and the 180-deg conformers so the 90-deg conformer becomes the lowest in energy when this interaction is replaced by hyperconjugation with C–H bonds.

In summary, the current study showed that all fragment ions examined (**3**, **4**, and **5**) display more than one stable conformation. The barrier heights for interchange between these conformers are calculated to be rather low using both hybrid density functional theory methods employed here. This implies that all cation conformations are available at room temperature, and that they are easily interchangeable. It is therefore unlikely that the difference in the fragmentation pathways observed in the mass spectroscopy of the diastereoisomers of dioxanes derivatives **1** and **2** is due to the existence of these isomeric ions. It is quite possible though that the two diastereoisomers of **1** or **2** will generate, during the fragmentation process, the same pair of carbocations (**3** and **4** or **3** and **5**) in different excited vibrational states leading to different reactivities (or stabilities). The same idea was postulated by Loutelier-Bourhis *et al.*,<sup>16</sup> but the authors attributed the different reactivities for these ions to different isomeric ions (i.e., conformers). Additional experimental and/or theoretical studies could provide further insight or could reveal other factors that might be significant to this subject.

## CONCLUSIONS

This paper presents the conformational analysis of some carbocations formed as intermediates in the mass spectrometry of diastereoisomers of 1,3-dioxane derivatives **1** and **2**. We found that each ion examined had more than one stable conformer. Cation **3** shows two distinct conformations separated by a very small barrier height implying easy

interchange between the two conformations. For cations **4** and **5** we found three different stable conformations. There is, however, a difference in the most stable conformer of **4** and **5**; the lowest-energy conformer for **4** has  $C_s$  symmetry while the lowest-energy conformer for **5** has  $C_1$  symmetry. Due to the relatively small rotation barrier height, the different conformers are unlikely to be involved in distinct fragmentation pathways leading to different EI mass spectra unless they are generated in different vibrationally excited states therefore displaying different reactivities.

### Acknowledgements

The author appreciates the support in carrying out this research provided by the College of Arts and Sciences at Tennessee Technological University.

### SUPPLEMENTARY INFORMATION

The Supplementary Information includes geometries in Cartesian coordinates for all structures of stationary points optimized in this work.

### REFERENCES

- Harrison AG. *Chemical Ionization Mass Spectrometry* (2nd edn). CRC Press: Boca Raton, 1992.
- Splitter JS, Turecek F. *Applications of Mass Spectrometry to Organic Stereochemistry*. VCH: New York, 1994.
- Van de Sande CC, Van Gaever F, Sandra P, Monstrey J. *Naturforsch Z.* 1977; **32B**: 573.
- Van de Sande CC, Van Gaever F, Hanselaer R, Vandewalle M. *Naturforsch. Z.* 1977; **32B**: 810.
- Van Gaever F, Monstrey J, Van de Sande CC. *Org. Mass Spectrom.* 1977; **12**: 200.
- Suming H, Yaozu C, Longfei J, Shuman X. *Org. Mass Spectrom.* 1985; **20**: 719.
- Chen Y, Li H, Yang H, Hua S, Li H, Zhao F, Chen N. *Org. Mass Spectrom.* 1988; **23**: 821.
- Gervat V, Fournier F, Perlat M-C, Tabet J-C. *J. Am. Soc. Mass Spectrom.* 1997; **8**: 610.
- Rathahao E, Perlat MC, Fournier F, Tabet J-C. *Int. J. Mass Spectrom.* 1999; **193**: 161.
- Mancel V, Sellier N. *Rapid Commun. Mass Spectrom.* 2000; **14**: 80.
- Mancel V, Sellier N, Lesage D, Fournier F, Tabet J-C. *Adv. Mass Spectrom.* 2001; **15**: 717.
- Da Silva Marina V, Perlat M-C, Tabet J-C, Giorgi G, Salvini L, Ponticelli F. *J. Am. Soc. Mass Spectrom.* 2003; **14**: 851.
- Mancel V, Sellier N, Lesage D, Fournier F, Tabet J-C. *Int. J. Mass Spectrom.* 2004; **237**: 185.
- Green MM. In *Topics in Stereochemistry*; vol. 9. John Wiley: New York, 1976; 35.
- Munson B, Jelus BL, Hatch F, Morgan TK Jr, Murray RK Jr. *Org. Mass Spectrom.* 1980; **15**: 161.
- Loutelier-Bourhis C, Balog M, Grosu I, Ramondenc Y, Ple G, Lange CM. *Rapid Commun. Mass Spectrom.* 2005; **19**: 1644.
- Rauk A, Sorensen TS, Maerker C, de Carneiro JW, Sieber S, Schleyer PvR. *J. Am. Chem. Soc.* 1996; **118**: 3761.
- Kirchen RP, Sorensen TS. *J. Am. Chem. Soc.* 1978; **100**: 1487.
- Alabugin IV, Manoharan M. *J. Org. Chem.* 2004; **69**: 9011.
- Perdew JP, Chevary JA, Vosko SH, Jackson KA, Pederson MR, Singh DJ, Fiolhais C. *Phys. Rev. B* 1992; **46**: 6671.
- Adamo C, Barone V. *J. Chem. Phys.* 1998; **108**: 664.
- Lynch BJ, Fast PL, Harris M, Truhlar DG. *J. Phys. Chem. A* 2000; **104**: 4811.
- Frisch MJ, Trucks GW, Schlegel HB, Scuseria GE, Robb MA, Cheeseman JR, Montgomery JA Jr, Vreven T, Kudin KN, Burant JC, Millam JM, Iyengar SS, Tomasi J, Barone V, Mennucci B, Cossi M, Scalmani G, Rega N, Petersson GA, Nakatsuji H, Hada M, Ehara M, Toyota K, Fukuda R, Hasegawa J, Ishida M, Nakajima T, Honda Y, Kitao O, Nakai H, Klene M, Li X, Knox JE, Hratchian HP, Cross JB, Bakken V, Adamo C, Jaramillo J, Gomperts R, Stratmann RE, Yazyev O, Austin AJ, Cammi R, Pomelli C, Ochterski JW, Ayala PY, Morokuma K, Voth GA, Salvador P, Dannenberg JJ, Zakrzewski VG, Dapprich S, Daniels AD, Strain MC, Farkas O, Malick DK, Rabuck AD, Raghavachari K, Foresman JB, Ortiz JV, Cui Q, Baboul AG, Clifford S, Cioslowski J, Stefanov BB, Liu G, Liashenko A, Piskorz P, Komaromi I, Martin RL, Fox DJ, Keith T, Al-Laham MA, Peng CY, Nanayakkara A, Challacombe M, Gill PMW, Johnson B, Chen W, Wong MW, Gonzalez C, Pople JA. *Gaussian 03, Revision D.01*, Gaussian, Inc.: Wallingford, CT, 2004.
- Lynch BJ, Truhlar DG. *J. Phys. Chem. A* 2001; **105**: 2936.
- Albu TV, Lynch BJ, Truhlar DG, Goren AC, Hrovat DA, Borden WT, Moss RA. *J Phys. Chem. A* 2002; **106**: 5323.
- Coote ML. *J. Phys. Chem. A* 2004; **108**: 3865.
- Andersson S, Gruening M. *J. Phys. Chem. A* 2004; **108**: 7621.
- Albu TV, Corchado JC, Truhlar DG. *J. Phys. Chem. A* 2001; **105**: 8465.
- Zuev PS, Sheridan RS, Albu TV, Truhlar DG, Hrovat DA, Borden WT. *Science* 2003; **299**: 867.
- Carey FA, Sundberg RJ. *Advanced Organic Chemistry* (4th edn). Kluwer Academic/Plenum Publishers: New York, 2000.